Kochi Chapter

Indian Geotechnical Conference
IGC 2022
15th – 17th December, 2022, Kochi

A Critical Review on Static and Seismic Earth Pressure of Layered Soil on Retaining Wall

Siddalingeshwara D H[1] and Kaustav Chatterjee[2]
[1] Research Scholar, Department of Civil Engineering, Indian Institute of Technology, Roorkee-247667
siddalingeshwara_h@ce.iitr.ac.in
[2] Assistant Professor, Department of Civil Engineering, Indian Institute of Technology, Roorkee-247667
kaustav.chatterjee@ce.iitr.ac.in

Abstract. Retaining walls are usually constructed to retain the backfill soil. However, a seismic study of earth pressure in layered soils is complicated and cannot be reliably predicted due to soil-structure interaction influenced by the backfill soil properties and wall rigidity. The complexity lies in understanding the potential failure surface and the soil arching effects due to the interaction of the soil layers. It is observed that the possible failure surface in the backfill soil depends upon the friction angle between the wall and backfill soil. The failure surface tends to be planar for small friction angles, and a curved failure surface is observed for higher friction angles. Also, under pseudo-static conditions with constant seismic coefficients, the stress distribution in soil along the height of the retaining wall presents a non-linear pattern approaching a curvilinear surface behind the retaining wall in the active and passive case. Moreover, the effect of non-homogeneity due to the layered soils leading to the soil arching phenomenon due to the interaction of soil layers on the distribution of earth pressure is also a concern. This paper describes the distribution of earth pressure in layered c-phi soil, considering the effect of the soil arching phenomenon.

Keywords: Retaining wall; Arching effect; Layered soil; Seismic

1 Introduction

The earth pressure behind the rigid retaining walls dominates the design and construction of retaining walls. It is of utmost importance to consider suitable theoretical and practical parameters related to the stability of the walls for safe and durable construction. The backfills of these walls may be cohesionless, cohesive, or generalized depending upon the natural conditions leading to the variation in the earth pressure coefficient along the height of the retaining wall. However, the seismic effects are more vulnerable in the case of layered soils behind the retaining walls. Earth pressure is generally estimated using Rankine's theory (1857) and Coulomb's theory (1776), which are based on limit-state analyses. Also, Coulomb's approach is based on the assumption that the failure soil wedge slips along a linear surface passing through the heel of the wall, which overestimates the passive earth pressure when the wall friction angle is greater than one-third of the soil friction angle. Okabe (1926) and Mononobe-Matsuo (1929) conducted shake table tests leading to the limit equilibrium force-based approach, an extension of Coulomb's theory, which is based on the pseudo-static earthquake loading for cohesionless soils by applying horizontal and vertical acceleration coefficients, but the use of seismic coefficients is largely empirical leading to inconsistent, conservative and unsafe design. Seed and Whitman (1970) expressed the total maximum earth pressure into two components, i.e., initial static pressure on the wall and the dynamic pressure increment due to the base motion such that the resultant dynamic thrust acts at 0.6h from the base of the wall, unlike M-O theory. Also, they suggested that the effect of the horizontal acceleration component is higher compared to the vertical acceleration component, which can be neglected for practical purposes. Richards and Elms (1979) presented a rational method for selecting a suitable seismic coefficient based on the concept of allowable permanent displacement following Newmark's sliding block analysis (1965) and suggested a liberal safety factor to accommodate the uncertainties in the study. However, all the above methods use simple exact form solutions with simplicity in geometry, material behavior, or dynamic loading to make the equations solvable. It is to be noticed that the formulations made by the above theories were derived by assuming a planar failure surface. In general, planar failure surfaces overestimate passive pressures and might underestimate active pressure. Morrison and Ebeling (1992) considered log-spiral failure surface to determine passive earth pressure, which was more generalized than planar failure surface. Extensive experimental observations and theoretical analysis have clearly indicated that the most critical sliding surface is curved and the earth pressure is overestimated with the planar failure surface. Also, to overcome the limitation of the

pseudo-static method, Steedman, and Zeng (1990) proposed a pseudodynamic approach to estimate seismic active earth pressure by considering time and phase difference caused by finite shear wave propagation behind a retaining wall. Choudhury and Nimbalkar (2005) extended the pseudodynamic method by considering the effect of vertical seismic acceleration in terms of primary wave velocity for the estimation of seismic passive earth pressure and later extended this work for the estimation of seismic active earth pressure. Ghosh et al. (2010) presented analytical expressions for earth pressure by the pseudodynamic method for non-vertical retaining walls. Shukla et al. (2011) presented analytical expressions for determining active and passive earth pressure with surcharge under seismic load. Rajesh et al. (2016) and Pain et al. (2017) adopted a modified pseudodynamic approach for determining active and passive earth pressure respectively. However, it is observed that the seismic study on retaining walls with layered cohesive frictional soil is very limited and is therefore discussed in the present study.

1. Limit equilibrium analysis

Shi et al. (2016) proposed this method to predict the static and dynamic earth pressure against sliding and overturning for c-phi soils with surcharge. The analysis is entirely based on geometry, unlike the conventional method for calculation as it becomes complicated under layered soil. The soil failure wedge was divided into a thin layer of micro-elements such that the resulting failure surface as a whole was curved. This method is assumed to be different from the conventional horizontal method of slices in two ways. Firstly, the rupture angles of individual micro-element were assumed to vary depending on maximizing the total force for active earth pressure or minimizing the total force for passive earth pressure. Secondly, the retaining wall stability was assumed to depend on the moments resulting from the active or passive earth pressure but not the forces alone for the overturning condition. Limit equilibrium analysis was adopted for the determination of the earth pressure in this study.

1.1 Static Active earth pressure

A retaining wall with height h, as shown in Fig 1(a), with layered soil having an inclination angle of the wall with vertical, α, unit weight, γ_i, internal friction angle, Φ_i, friction angle between wall and backfill δ_i, and the soil cohesion c_i, was considered. The subscript i represents the ith soil layer. AD is the horizontal ground surface with a uniform surcharge q_0.

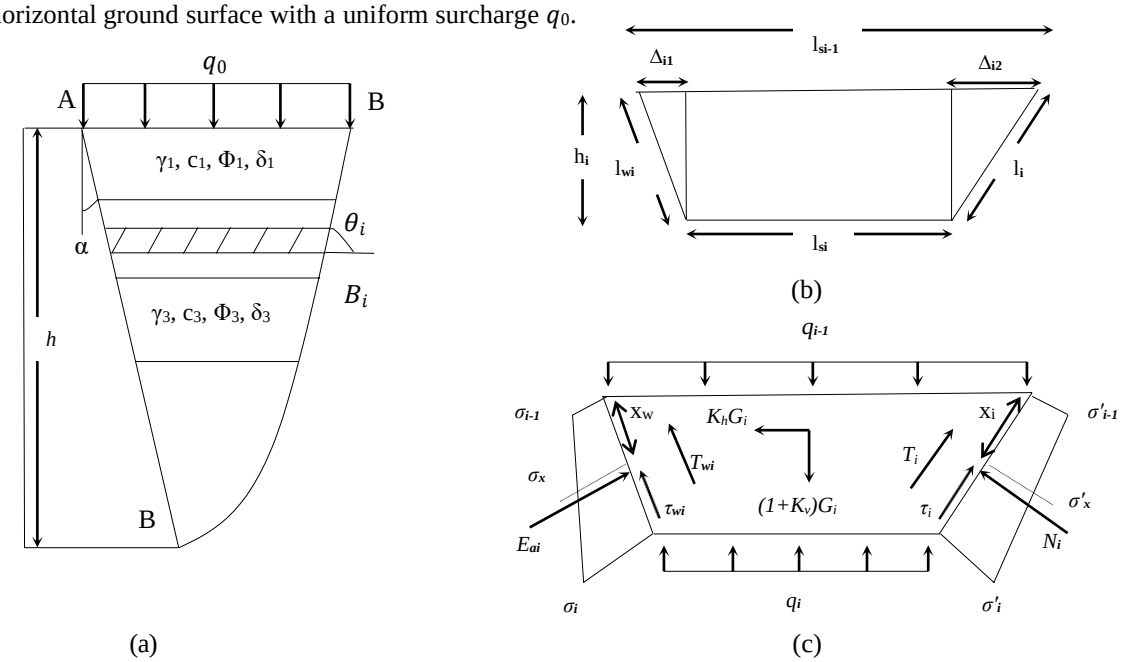

Fig 1 (a) Soil wedge and the retaining structure (b) Geometric dimensioning of the micro-element (c) Force diagram of the microelement under active case (Shi et al. 2016).

Due to the surcharge load and the self-weight of the individual element layers, a failure surface is assumed to extend from the heel of the wall to the backfill, thus forming a failure wedge. The shear resistance of the slip surface would be fully mobilized with the assumption that the wall has moved

sufficiently; the corresponding force associated is called active earth pressure. Now to determine the active earth pressure, after dividing the soil wedge into n micro-elements, the slip surface in each micro-element was assumed to be planar for the analysis. $DB_1B_2 \ldots B_n$ in Fig 1(a) was the potential slip surface. The soil failure wedge was not divided equally so as to simulate the natural soil layer and its homogeneity. A quadrangle micro-element with thickness h_i was selected from the sliding wedge for the limit equilibrium analysis to determine the earth pressure, as shown in Fig 1(b). l_{wi}, l_i, l_{si-1}, l_{si} are the lengths of the micro-element along the wall, slip surface, top surface, and bottom surface. Forces acting on the i^{th} micro-element are shown in Fig 1(c) with uniform vertical pressures acting both on the top (q_{i-1}) and bottom of the element (q_i) and the stresses normal (σ_i) and tangential (r_i) to the back surface of the element.

The resultant active thrust, E_{ai} is calculated by integrating the stress σ_i along the length l_{wi}.

$$E_{ai} = \int_0^{l_{wi}} \sigma_x \, dx_w = \frac{1}{2}(\sigma_{i-1} + \sigma_i) l_{wi} \quad (1)$$

$$\sigma_i = \frac{J - D + F*A}{C - E - F*B} \quad (2)$$

$$\sigma_i' = B * \frac{J - D + F*A}{C - E - F*B} + A \quad (3)$$

$$q_i = C * \frac{J - D + F*A}{C - E - F*B} + D \quad (4)$$

$$G_i = G_{i1} + G_{i2} + G_{i3} \quad (5)$$

$$G_{i1} = \frac{\gamma_i \Delta_{i1} h_i}{2} \qquad G_{i2} = \gamma_i h_i l_{si} \qquad G_{i3} = \frac{\gamma_i \Delta_{i2} h_i}{2} \quad (6)$$

where A, B, C, D, E, F and J are the parameters which depends upon the geometric properties of the soil micro-element. The above recursive equations 2, 3, 4 were used to determine the stresses on the micro-elements which is a function of weight of soil G_i calculated using equations 5 and 6, surcharge q_0, external friction angle δ_i, soil cohesion c_i, internal friction angle Φ_i, and rupture angle θ_i. Δ_{i1} and Δ_{i2} are the lengths of the horizontal projection for the two bevel edges of the i^{th} micro-element determined using the geometry. To determine the earth pressure, terms σ_1, σ_1', q_1 are determined by considering the first soil layer (i= 1) by using the above equations 2, 3, 4 based on q_0 and then σ_{i+1}, $\sigma_{i+1}' q_{i+1}$ are determined based on σ_1, σ_1' and q_1. It is to be noted that (σ_1, σ_1', q_1), (σ_2, σ_2', q_2)…., (σ_n, σ_n', q_n) are calculated based on given values of θ_1, θ_2,… θ_n. For active case, to calculate the maximum active pressure causing the wall to thrust or overturn, optimization method was adopted to determine the rupture angle corresponding to maximum thrust or overturn. θ_1, θ_2,… θ_n determined after optimization for a maximum value, yields a curved rupture surface while if $\theta_1 = \theta_2 = \ldots = \theta_n = \theta$, a planar rupture slip surface was assumed to be obtained.

1.2 Static Passive earth pressure

The passive earth pressure was determined using similar recursive formulae as used for the active earth pressure, but the direction of the stresses r_{wi}, r_i would be acting in the opposite directions to those denoted in Fig 1(c). Again, similar optimization method was used to determine the rupture angle corresponding to minimum thrust or overturn leading to the determination of passive earth pressure.

1.3 Dynamic Active Earth Pressure

A seismic horizontal inertia force $k_h G_i$ and vertical force $k_v G_i$, were considered for the analysis, where k_h and k_v represent the horizontal and vertical acceleration coefficients. From equilibrium analysis of the element shown in Fig 1(c), expressions σ_i, q', q_i for the seismic active earth pressure are derived as shown in equations below, the procedure to calculate dynamic active earth pressure is same as that for the static active earth pressure

$$\sigma_i = \frac{B + BB*B + CC - E}{C - A + D*(AA + BB*A)} \quad (7)$$

$$\sigma_i' = A * \frac{B + BB*B + CC - E}{C - A + D*(AA + BB*A)} + B \quad (8)$$

$$q_i = (AA + BB * A) * \frac{B+BB*B+CC-E}{C-A+D*(AA+BB*A)} + BB * B + CC \quad (9)$$

1.4 Dynamic Passive Earth Pressure

The passive earth pressure was determined based on the similar recursive formulae as used for the dynamic active earth pressure, but the direction of the stresses r_{wi}, r_i would be acting in the opposite directions to those denoted in the Fig 1(c) other aspects being same. Authors concluded that, the earth pressures calculated with this method were in good agreement with Rankine's, Coulomb's, Mononobe-Okabe's theory and the experimental studies conducted by Fang [3] and the magnitude of active earth pressure predicted for the case of curved failure surface was slightly higher than that predicted for planar failure mechanism. It was observed that, when the external friction angle between soil backfill and wall (δ=0) is zero, the stress distribution was linear, and planar failure surface was obtained; a curved failure surface was obtained when (δ≠0), with earth pressure distribution being curvilinear in nature.

2. Slip line method

F. Q. Liu (2014) proposed this method to determine axi-symmetric active earth pressure under static condition in levelled layered backfill soils for the circular retaining walls subjected to a uniformly distributed load q on the ground surface. The author extended Berezantzev's results to the layered soils following a slip line theory which involves a network of slip lines known as slip-line field, which is bounded by regions, which are rigid. These slip lines are constructed in the vicinity of the structure as shown in Fig 2(b) which represents the directions of maximum shearing stresses. In case of plane strain problems, there are two differential equations of plastic equilibrium and a yield condition available for solving the three unknown stresses, these equations are written with respect to curvilinear coordinates that coincide with slip-lines. If the wall boundary conditions are given only in terms of stresses, these equations are sufficient to give the stress distribution without any reference to the stress-strain relationship.

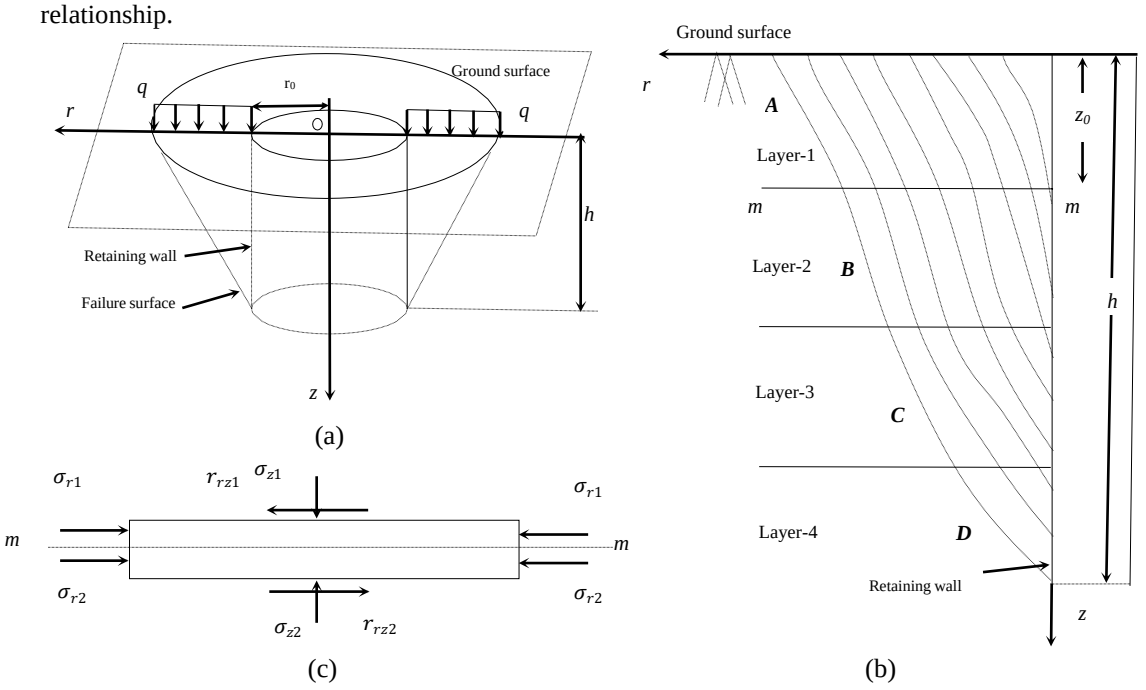

Fig 2 (a) Problem model of the domain (b) Slip line field for layered backfill (c) Stress state of the soil element at the interface of two soil layers (F. Q. Liu 2014).

The problem model is as shown in Fig 2(a). The backfill soil had two layers such that the interface behaves as a stress discontinuous surface as on both sides of the interface, the soil properties are different. The origin of the co-ordinate system 'O' is defined as the center of the section on the ground surface. The vertical *z*-axis with downward positive direction and *r*-axis in the radial direction have r_0

and h as the radius and the depth of the excavation. Only *r-z* plane was analyzed due to axi-symmetry formulation. Layered backfill with an interface *m-m* was considered for the analysis, z_0 being the thickness of the top layer, with *h* as the height of the retaining wall. $\sigma_r,\ \sigma_z\ and\ r_{rz}$ are the stress components. The stress components of a soil element satisfying the equilibrium equations are as follows

$$\frac{\partial \sigma_r}{\partial r}+\frac{\partial c_{rz}}{\partial z}+\frac{\sigma_r-\sigma_\theta}{r}-G=0 \qquad \frac{\partial c_r}{\partial r}+\frac{\partial \sigma_z}{\partial z}+\frac{c_{rz}}{r}-H=0 \tag{10}$$

where, $\sigma_r,\ \sigma_\theta,\ \sigma_z\ and\ r_{rz}$ are the stress components, G and H are the radial and vertical components of the body force, respectively. From Mohr's circle, representing the stress state of a point, the stress components were written as (Berezantzev 1952)

$$\sigma_r=\sigma(1+sin\Phi cos2\psi)-ccot\Phi \quad \sigma_z=\sigma(1-sin\Phi cos2\psi)-ccot\Phi \quad r_{rz}=\sigma sin\Phi sin2\psi \tag{11}$$

$$\sigma_\theta=\lambda\sigma_1=\lambda[\sigma(1+sin\Phi)-ccot\Phi] \tag{12}$$

The mean stress $\sigma=\frac{\sigma_1-\sigma_3}{2sin\Phi}=\frac{\sigma_1+\sigma_3}{2}+ccot\Phi$ (13)

where $\sigma_1,\ \sigma_3$ = major and minor principal stresses; c, Φ = cohesion and internal friction angle of soil; ψ = angle of major principal stress σ_1 inclined to r-axis. λ is the tangential stress coefficient and is controlled by amount of wall movement. At an active state, $\lambda = 1$ (Cheng et al. 2007); if the wall has no displacement, $\lambda = K_0$. In this paper, the relationship between, λ and the wall movement was considered and given by

$$\lambda=\frac{4}{\pi}tan^{-1}\frac{s}{s_a}(1-K_0)+K_0, \qquad s\leq s_a \tag{14}$$

where, s is the wall displacement, Φ_0 is the initial angle of internal friction, $\Phi_0=arcsin(\frac{1-K_0}{1+K_0})$ where, $K_0=1-sin\Phi$ for a normally consolidated sand. $\Phi_{mob}=\Phi_0$ at *s*=0 and $\Phi_{mob}=\Phi$ at *s*=s_c, which means that the angle of wall friction of soil is fully mobilized when wall movement reaches s_c . Cheng (1997) concluded that the active state occurs when wall friction attains its maximum value, and the wall movement needed is denoted as s_c , (s_c~0.03%*h*, *h*- height of the retaining wall) and lateral earth pressure cannot attain a minimum value when *s*=s_c, a larger displacement is needed, denoted as s_a, ($s_a=0.1-0.5\%h$). In the present work, the author considered the major principal direction ($\psi=\pi/2$) in the whole slipping region, and the slip lines as a group of polygonal lines as shown in Fig 2(b). Φ_{mob} depends on the movement of the intersection point of slip lines and wall back and was obtained by the equation below.

$$\Phi_{mob}=tan^{-1}[tan\Phi_0+\frac{s}{s_c}(tan\Phi-tan\Phi_0)] \tag{15}$$

A generalized equation was developed by substituting equation 11 and 12 into equation 10, which yields hyperbolic type differential equation. This equation was solved by iterative relationships following Berezantzev's procedure leading to following generalized equation as shown below

$$\frac{d\sigma}{dr}+\frac{\sigma}{r}tan(\frac{\pi}{4}+\frac{\Phi}{2})[\frac{sin\Phi(1+\lambda)-(1-\lambda)}{cos\Phi}]=0 \tag{16}$$

On solving, $\sigma=Cr^m+\frac{Tr}{m-1}$ (17)

Above equation determines the mean stress on a slip line, where *C* is the integration constant obtained from boundary conditions. *T* and *m* satisfy the following equations

$$m=tan(\frac{\pi}{4}+\frac{\Phi_{mob}}{2})[\frac{sin\Phi_{mob}(1+\lambda)-(1-\lambda)}{cos\Phi_{mob}}] \quad ; \quad T=\frac{\gamma}{cos\Phi_{mob}} \tag{18,19}$$

On the ground surface, normal stress is q, and the mean stress on the ground surface at A was given by

$$\sigma_A=\frac{q}{1+sin\Phi_{mob}} \tag{20}$$

From equations 17 and 20, value of *C* was determined and resubstituted into equation 17, the mean stress on the wall at point B was determined and is as given below

$$\sigma_B = \left(\frac{q}{1+sin\Phi_{mob}} - \frac{Tr_A}{m-1}\right)\left(\frac{r_0}{r_A}\right)^m + \frac{Tr_0}{m-1} \quad (21)$$

On the interface as shown in Fig 2(c), σ_z and r_{rz} would be continuous if equations 19 and 20 would be satisfied

$$\sigma_{z1} = \sigma_{z2} \qquad r_{rz1} = r_{rz2} \quad (22)$$

$$\left.\begin{aligned}\sigma_1(1 - sin\Phi_1 cos2\psi_1) &= \sigma_2(1 - sin\Phi_2 cos2\psi_2)\\ \sigma_1(sin\Phi_1 sin2\psi_1) &= \sigma_2(sin\Phi_2 sin2\psi_2)\end{aligned}\right\} \quad (23)$$

The parameters with subscript 1 represent the upper side of the interface, and subscript 2 represents the lower side of the interface. It was considered that, $\psi_1 = \psi_2 = \pi/2$, which means that the mean stresses on both sides of the interface satisfy

$$\sigma_2 = \sigma_1 \frac{(1+sin\Phi_1)}{(1+sin\Phi_2)} \quad (24)$$

For layered backfill as in Fig 2(b), equation 21 gives the mean stress on the upper side of point B as

$$\sigma_B^+ = \left(\frac{q}{1+sin\Phi_{mob1}} - \frac{T_1 r_A}{m_1-1}\right)\left(\frac{r_B}{r_A}\right)^{m_1} + \frac{T_1 r_B}{m_1-1} \quad (25)$$

where Φ_{mob1} is the mobilized angle of internal friction on slip line in layer 1; m_1 and T_1 are determined using equations 18 and 19. m_i and T_i (i=2,3) are obtained by analogy. Based on equation 24 and by using the result of equation 25, σ_B^- was determined as shown below in equation 26

$$\sigma_B^- = \sigma_B^+ \frac{(1+sin\Phi_{mob1})}{(1+sin\Phi_{mob2})} \quad (26)$$

$$\sigma_c^+ = \left(\sigma_B^- - \frac{T_2 r_B}{m_2-1}\right)\left(\frac{r_c}{r_B}\right)^{m_2} + \frac{T_2 r_C}{m_2-1} \quad (27)$$

$$\sigma_C^- = \sigma_C^+ \frac{(1+sin\Phi_{mob2})}{(1+sin\Phi_{mob3})} \quad (28)$$

$$\sigma_D = \left(\sigma_C^- - \frac{T_3 r_C}{m_3-1}\right)\left(\frac{r_0}{r_C}\right)^{m_3} + \frac{T_3 r_0}{m_3-1} \quad (29)$$

On obtaining the radial coordinates r_A , r_B , and r_C the mean stresses for layered backfill can be obtained. Thus, by analogy earth pressure at any depth on the wall would be determined. The obtained results were then compared with the finite element method proposed by Wang et al. (1997) and good agreement was observed with the measured data. The author concluded that, the earth pressure decreases exponentially with increase in the wall movement and h/r_0 value.

Discussions and Conclusions

The shape of the failure surface plays a critical role in determining the magnitude of lateral stresses and its point of application. In the above two methods, the authors have not considered the effect of soil arching which leads to stress redistribution by which stress is transferred around the zone of soil mass which in turn reduces the stresses on it. Goel S et al. (2008) conducted an analytical study on the effect of soil arching on rigid retaining wall considering a cohesionless soil and expressed active earth pressure as

$$\bar{\bar{\sigma}}_{ahw} = \left(\frac{\gamma H K_{awn}}{1 - K_{awn} tanatan\delta}\right)\left[(1 - z/H)^{K_{awn} tanatan\delta} - (1 - z/H)\right] \quad (30)$$

where, $K_{awn} = \dfrac{[cos^2\theta + (1/N)sin^2\theta]}{\{(1-cos\theta)[1+0.5cos\theta-(1/N)(1+0.5cos\theta+\frac{log(1-cos\theta)}{cos\theta}]\}}$ (31)

and N = $tan^2(45 + \frac{\Phi}{2})$, θ is the angle of minor principal stress plane with respect to the horizontal at the wall. it is to be noted that $\theta = 90°$ for $\delta = 0°, \Phi$ is the angle of internal wall friction.

In this paper, a comparison study is made to determine the active earth pressure. For simplicity in comparison, the active earth pressure is determined under static case for the same set of parameters such as height of retaining wall, h = 6m, surcharge load, q = 0 kN/sqm, inclination angle of the wall with

vertical, $\alpha = 0°$, soil wall friction angle, $\delta = 0°$, cohesion, c=0 kN/sqm, thickness and unit weight of the soil for layer 1 and layer 2 are h_1=1m, h_2= 2m, γ_1=16.5 kN/cum, γ_2=18 kN/cum respectively. The active thrust from the limit equilibrium analysis yielded a value of 84.9 kN/m, which is in agreement with the result obtained from Rankine's theory as 85.3 kN/m. Slip line method being completely different in the approach for the analysis from the former method yielded a value of 84 kN/m approximately. However, the above methods had not considered the effect of soil arching, which yields a value of 49.5 kN/m calculated using equation (30). The reduction in the active thrust is due to transfer of stresses to the surrounding soil. The two methods cannot be directly compared due to their way of approach in analysing the problem domain considering the phenomenon of soil arching but is done for the justification.

In limit equilibrium analysis, the assumption of failure slip surface being planar and curvilinear is vague. The method being pseudostatic does not cover the criteria for the selection of seismic coefficients.

In the slip line method, there is no advantage of including cohesion in the calculation of active earth pressure directly.

Both the methods discussed above does not consider tension crack in the analysis which affects the magnitude of active earth pressure. Limited studies have been conducted in layered cohesive frictional soils and there is a lack of experimental and numerical evidences for comparison and validation, therefore a detailed study for the seismic analysis in layered cohesive frictional soils is a scope for the future.

References

1. Berezantzev V. G., Axially symmetrical limit equilibrium problems of loose materials (soil) [M]. Moscow: Gostekhizdat Brinch Hansen, (1952).
2. Coulomb CA. Essais sur une application des regles des maximis et minimis a quelques problems de statique relatits a l'architecture. Mem Acad Roy Pres Divers Sav, (7) 343–82, (1776).
3. Choudhury, D., Nimbalkar, S., Seismic passive resistance by pseudodynamic method, Geotechnique (55), 699–702, (2005).
4. Cheng, Y M., Hu, Y Y., Wei, W B., General axisymmetric active earth pressure by method of characteristics-theory and numerical formulation, International Journal of Geomechanics, 7(1), 1-15, (2007).
5. Fang, Y S., Ho, Y C., Chen, T J., Passive earth pressure with critical state concept, Journal of Geotechnical and Geoenvironmental Engineering, 128(8), 651-659, (2002).
6. F Q, Liu., J H, Wang., A generalized slip line solution to the active earth pressure on circular retaining walls, Computers and Geotechnics, (35), 155-164, (2007).
7. F Q, Liu., Lateral earth pressure acting on circular retaining walls, International Journal of Geomechanics, 14(3), (2014).
8. Goel, S., Patra, N R., Effect of arching on active earth pressure for rigid retaining walls considering translation mode, International Journal of Geomechanics, 8(2), 123-133, (2008).
9. Ghosh. S., Pseudo-dynamic active force and pressure behind battered retaining wall supporting inclined backfill, Soil Dynamics and Earthquake Engineering, (30), 1226–1232, (2010).
10. Ghosh. S., Saha A., Nonlinear failure surface and pseudodynamic passive resistance of a battered-faced retaining wall supporting c-φ backfill., International Journal of Geomechanics, 1-9, (2014).
11. Mononobe, N., Matsuo, H., On the determination of earth pressure during earthquakes., In: Proceedings of world engineering conference, (9), 179– 187, (1929).
12. Morrison, Jr., EE, Ebeling, RM., Limit equilibrium computation of dynamic passive earth pressure, Canadian Geotechnical Journal, 32(3), 481–487, (1995).
13. Okabe S., General theory of earth pressure., Journal of Japan Society of Civil Engineers, 12(1), 311, (1926).
14. Pain, A., Choudhury, D., Bhattacharyya, S K., Seismic passive earth resistance using modified pseudo-dynamic method, Earthquake Engineering and Engineering Vibration, 16(2), 263-274, (2017).
15. Rankine, W J M., On the stability of loose earth. Philos Trans R Soc Lond, 147 (Part 1), 9–27 (1857).
16. Richards, R., Elms, D G., Seismic behavior of gravity retaining walls, ASCE Journal of Geotechnical Engineering Division, (105), 449-464, (1979).
17. Rajesh, B G., and Choudhury, D., Generalized seismic active thrust on a retaining wall with submerged backfill using a modified pseudodynamic method, International Journal of Geomechanics, 17(3), (2017).

18. Seed, H B., Whitman RV., Design of earth retaining structures for dynamic loads, In: Proceedings of ASCE specialty conference on lateral stresses in the ground and the design of earth retaining structures. Ithaca, NY: Cornell University New York, 103–47, (1970).
19. Steedman, R S., Zeng, X., The influence of phase on the calculation of pseudo-static earth pressure on a retaining wall, Geotechnique, (40), 103–12, (1990).
20. Shukla, S K., Dynamic active thrust from c-Φ soil backfills, Soil Dynamics and Earthquake Engineering., 31(3), 526–529, (2011).
21. Shi, H., Jinxing, G., Yanqing, Z., Earth pressure of layered soil on retaining structures, Soil Dynamics and Earthquake Engineering, (83), 33-52, (2016).
22. Singh, A., Kumar, A., Methodologies available for the determination of seismic active thrust acting on retaining walls: A critical review., 51(5), 1056-1068, (2021).
23. Wang S. H., Li W., Wang Y., A finite element simulation to the process of excavation of a circular retaining wall, China Harbour Engineering, 30-33 (1997).